Wide angle anapole excitation in stacked resonators

Vennberg, Felix ; Angelsten, Arvid; Anttu, Nicklas; Ravishankar, Ajith P.; Anand, Srinivasan

Published in:
Optics Express

DOI:
10.1364/OE.505539

Published: 01/01/2024

Document Version
Final published version

Document License
CC BY

Research Article Vol. 32, No. 3 / 29 Jan 2024 / Optics Express 4027
Optics EXPRESS

Wide angle anapole excitation in stacked resonators

FELIX VENNBERG,[1,*] ARVID ANGELSTEN,[1] NICKLAS ANTTU,[2] AJITH P. RAVISHANKAR,[1] AND SRINIVASAN ANAND[1]

[1]Applied Physics, School of Engineering Sciences, KTH Royal Institute of Technology, Stockholm, Sweden
[2]Physics, Faculty of Science and Engineering, Åbo Akademi University, FI-20500 Turku, Finland
[*]felixven@kth.se

Abstract: In the search for resonances with high localized field strengths in all-dielectric nanophotonics, novel states such as anapoles, hybrid anapoles and bound states in the continuum have been realized. Of these, the anapoles are the most readily achievable. Interaction between vertically stacked disks supporting anapole resonances increases the field localization further. When fabricated from materials with high non-linear coefficients, such stacked disk pillars can be used as non-linear antennas. The excitation of such 3D pillars often includes off normal incidence when using focusing optics. Therefore, it is important to evaluate the angular and polarization response of such pillars. In the paper we fabricate pillars with three AlGaAs disks in a stack separated by stems of GaAs. The angular and polarization responses are evaluated experimentally with integrating sphere measurements and numerically through simulation, multipole decomposition and quasi-normal modes. We find that the stacked geometry shows hybridized anapole excitation for a broad span of incidence angles, with tunability of the individual multipolar response up to octupoles, including an electric octupole anapole, and we show how the average enhanced confined energy varies under angled excitation. The results show that the vertical stacked geometry can be used with highly focusing optics for efficient in-coupling to the hybridized anapole.

1. Introduction

Resonance engineering in all-dielectric nanostructures has become a large field of study in recent years. The main goal is to confine the electromagnetic radiation to some desired region of space and time. The general drive has been to confine light to ever smaller material volumes and achieve higher field strengths. Higher field strengths increase light matter interaction which enhances absorption, optical non-linear effects, sensing capabilities and enables fabrication of more compact optical elements such as optical computers [1–6].

There is a wide variety of ways to confine light to small volumes. Most of the methods involve resonant states and their interactions with each other. The types of resonances and methods used include Mie, waveguides, photonic crystals, Fabry-Perot and array effects [7]. Of these, Mie resonances have received much attention recently. The development of fabrication, simulation and theoretical techniques has led to the establishment of "Mie-tronics" [8]. However, the optical confinement of individual Mie resonances are limited due to their leaky nature, especially compared to for example (bound) defect states in photonic crystals or whispering gallery modes in photonic ring resonators [9,10]. One way to increase the confinementof Mie resonant structures is through resonance engineering. By designing structures such that the resonances interfere with each other in specific ways, new types of optical states such as bound states in the continuum, anapoles and hybrid anapoles can be realized [11–14]. Higher Q-values can be achieved with arrangement of complex scatterers, that is with more than one scattering element. For example,

#505539 https://doi.org/10.1364/OE.505539
Journal © 2024 Received 13 Sep 2023; revised 3 Dec 2023; accepted 6 Dec 2023; published 23 Jan 2024

Optics EXPRESS

multiple dielectric disk resonators in axial systems can form hybridized resonances, as well as disks inside rings with coinciding anapole resonances [15–17].

The scattering response of Mie resonators is generally sensitive to the excitation conditions. For example, scatterers with broken symmetry behaves differently depending on the incidence angle and polarization of light. The most common response is a change in the amplitude and wavelength position of the individual resonances. Such changes can be detrimental when using carefully engineered states, in both simple and complex geometries that depend on interference of resonances.

Stacked or coaxial geometry enables more scatterers in a smaller area but requires supporting material to separate the individual resonators. A method of achieving optical separation is through under-etch of a sacrificial material. Multilayered III-V materials are suitable in this regard as there exists wet etchants with high selectivity and slow etch rates, enabling precise nanofabrication. In this paper we use a multilayer sample consisting of 50 nm AlGaAs and 100 nm sacrificial GaAs in three alternating layers on top of a GaAs substrate. To maximize the index contrast, in our work, the sacrificial GaAs layer is under-etched. The GaAs/AlGaAs material system is technologically mature with well-established fabrication processes. Additionally, AlGaAs is a suitable material for the resonators as it has one of the highest second order susceptibilities of all dielectrics, promising for efficient use in non-linear optical applications.

In a previous study we showed how stacked AlGaAs disks supporting electric dipole anapoles (EDA) hybridizes to significantly enhance the energy of the optical field inside the disks as compared to a single disk [18]. One application for these structures could be as non-linear optical antennas, since the strong field confinement is attractive for enhancing the efficiencies of non-linear optical processes.

In frequency conversion applications using non-linear processes, the excitation conditions could be important since most cases involve focusing optics, and thus a broad spectrum of incidence angles within the numerical aperture of the focusing optics. Then, to be able to excite the anapole state at a wide angle of incidence without compromising on wavelength position and field confinement of the resonance is vital to achieve as high efficiencies as possible. Though a few papers address the angle sensitivity in the context of absorption of a single disk supporting an EDA [12,19], most reports on anapolar states are restricted to vertical light incidence and angle and polarization dependence is rarely addressed [9,12,19,20]. Further, the stacked system with hybridized anapoles has not been investigated in terms of angle and polarization.

In this paper we show how a system of stacked III-V disks supporting hybridized anapoles evolves with incidence angle and polarization and employ multi-pole decomposition (MPD) and quasi-normal mode (QNM) analysis methods to explain the response. We find that the stacked geometry shows hybridized anapole excitation for a broad span of incidence angles, with tunability of the individual multipolar response up to octupoles, and we show how the average confined energy varies under angled excitation. The results show that these structures are efficient nanoantennas for a broad range of incidence angles that enables use with high NA objectives or use in off normal applications. For example, in non-linear optical applications (e.g. second harmonic generation and sum frequency generation) such an angle independent property where all the angles within the NA are populated is beneficial for efficient excitation of and collection of light from the resonant structures.

2. Methods

Fabrication

The pillars are fabricated from a multilayer wafer with 3 repetitions of alternating layers of 50 nm of $Al_{0.7}GaAs_{0.30}$ and 100 nm of GaAs on top of a GaAs substrate. As hard mask, 150 nm of SiO_2 is deposited via PECVD followed by a 30 nm thick Cr layer deposited using an e-beam evaporator. Charged polystyrene (PS) spheres are deposited with a method described in our

Optics EXPRESS

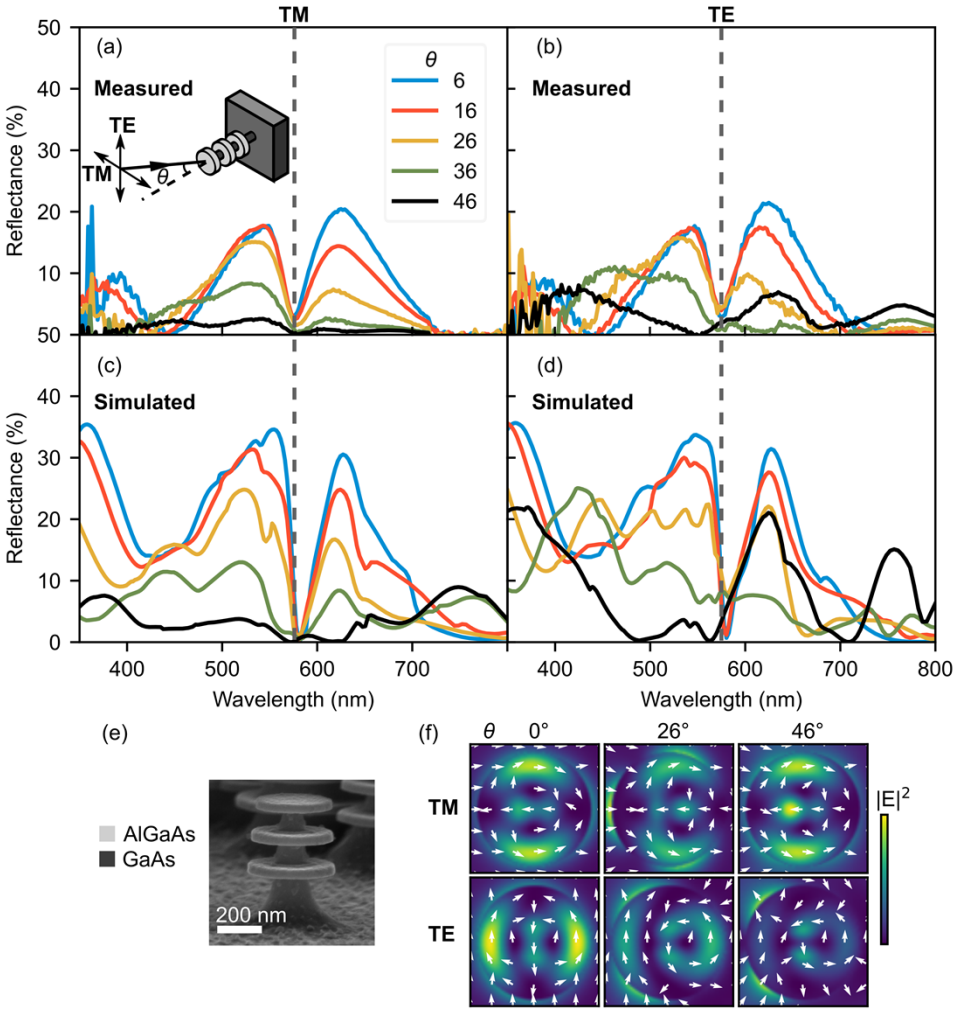

Fig. 1. (a)-(d) Measured and simulated specular reflectance as a function of incidence angle (degrees) and polarization for stacked disk pillars. The measured and simulated reflectance agree well. (e) SEM image of disk stack. (f) $|E|^2$ inside the middle disk for varying incidence angle, which show how the anapole pattern is distorted with angle and polarization. The white arrows display the field direction in the horizontal plane and are normalized to be of the same length.

previous paper [18]. The PS sphere pattern is transferred to the sample in an ICP-RIE, where the Cr is etched with Cl_2/O_2 plasma and the SiO_2 with CHF_3 chemistry. The III-V layers are etched with an Ar/Cl plasma in the same ICP-RIE. The hard masks are removed in HF (5%). The GaAs sacrificial layers is wet etched with a mixture of citric acid: H_2O_2, with a ratio of 20:1. More details are given in Ref. [18]. The final structure consists of three AlGaAs disks with diameter of 350 nm and height of 50 nm, separated by GaAs stems with diameter of 100 nm and height of 100 nm, see Fig. 1(e). The lateral distribution of the pillars is random but has a mean closest neighbour distance of about 600 nm.

Measurements

The specular reflectance with varying incidence angles was measured in an Agilent Cary 900 spectrophotometer with a Universal Measurement Accessory. The incident light is collimated

Optics EXPRESS

and directed onto the sample mount which can be rotated. A motorized detector collects light at twice the incidence angle to obtain the specular reflectance. The spot size was ~1 mm in diameter.

Simulations

FDTD simulations were performed with commercial software Lumerical FDTD. The refractive index was taken from Aspnes ($Al_{0.7}Ga_{0.3}As$) and from Palik (GaAs). For reflectance simulations, a period of 900 nm was used to avoid 1st order Wood-Rayleigh (WR) anomalies in the wavelength region of interest. Further, the period is sufficiently large to avoid near-field coupling between pillars, which is not present in the fabricated samples. A plane wave source was used. The disk diameters were 350 nm for the AlGaAs and 100 nm for the GaAs on top of a GaAs substrate. SCS, MPD, and average internal energy enhancement were obtained in simulations with three AlGaAs disks in air and no connecting stems. The mesh size for all simulations was 5 nm in every dimension. QNM was performed with COMSOL and a modified version of the package MAN [21].

3. Results

Figure 1(a-d) shows the measured and simulated specular reflectance for the stacked resonators as a function of incidence angle and polarization, for selected incidence angles of 6°, 16°, 26°, 36°, and 46°. There is a clear dip in specular reflectance at a wavelength of ~580 nm. The dip position exhibits angular independence up to 26 degrees for TE and 36 degrees for TM polarized excitation. However, the peaks on either side of the dip change with incidence angle—they flatten out for TM and gains additional peaks for TE polarization. The polarization dependence can qualitatively be explained through the cross-sectional field plots for the middle disk at the dip wavelength, seen in Fig. 1(f). All three disks show similar behaviour (see SI1) but the middle disk has the highest electric field concentration. At 6° off normal incidence the fields show characteristics of anapole-like excitation for both polarizations. With increased incidence angle, the fields become more asymmetric, especially for the TE polarization. Even though the fields are asymmetric, the wavelength of the dip does not change.

The FDTD simulations are for a periodic array of disk stacks, in square array, with a period of 900 nm, in which case WR anomalies did not show up in the spectra in the wavelength region of interest (as confirmed by test simulations with a slight variation of period to 850 and 950 nm). Measured and simulated spectra agree well even though the fabricated samples have a random distribution in the position of the disk stacks. This agreement strongly indicates that the reflectance dip associated with the anapole excitation does not depend on array properties and that there is no cross talk between pillars. The response is instead governed by the properties of a single pillar. A single pillar is more conveniently simulated as substrate free, illustrated in Fig. 2(a), where the response is given as the scattering cross section (SCS) rather than the reflectance. Such a system is easier to evaluate and analyse in-depth.

To evaluate complex scatterers, it is helpful to break down the scattering response. In this regard, MPD has become widely employed. It is a generalization of the vectorial spherical harmonics analytical solutions to the scattering of a dielectric sphere, but widened with computational techniques to arbitrarily shaped resonators [22,23]. The idea is to calculate the multipolar response from the induced current densities as excited by an electromagnetic source. The current density is retrieved through full numerical simulation of Maxwell's equations. Usually, it is enough to consider the first four terms of the expansion, -dipoles and -quadrupoles. However, for more complex geometries, higher order terms such as octupoles can be excited.

MPD gives the composition of the far-field scattered light but does not give intuitive understanding of the resonances excited within the structure. The vectorial spherical harmonics of Mie theory are only orthogonal for spherical particles, so that the resonances for a non-spherical scatterer may have contributions from several MPD components.

Optics EXPRESS

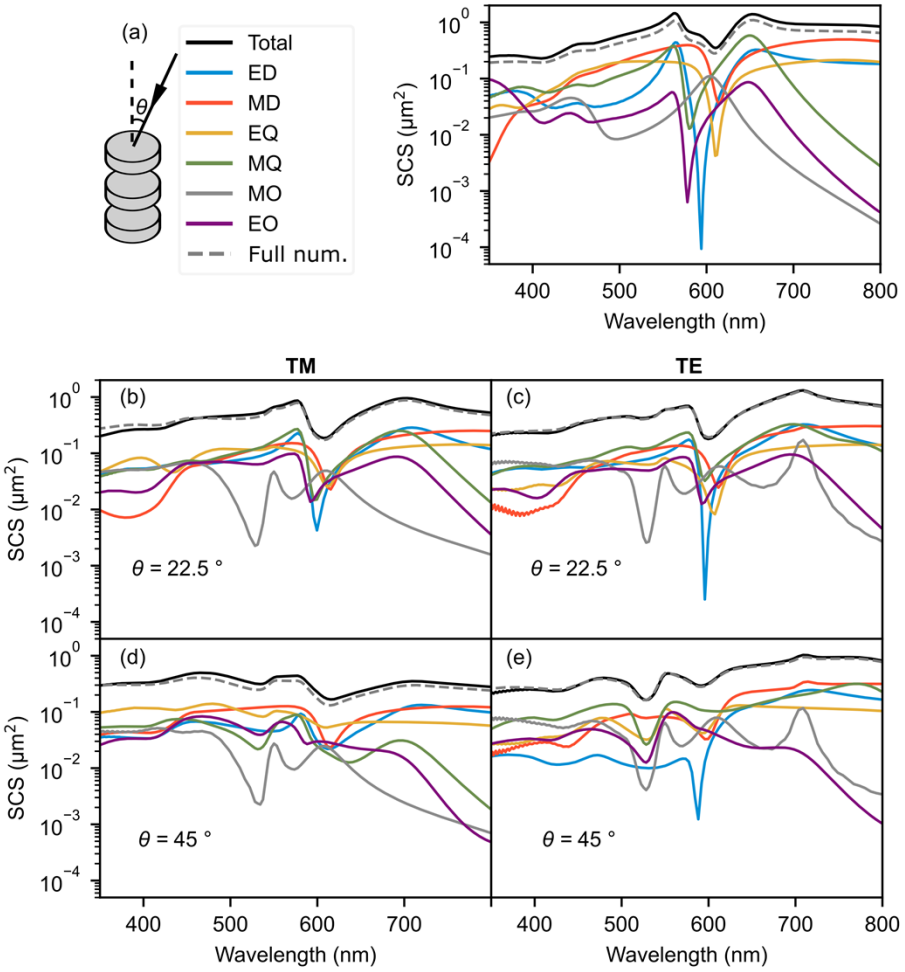

Fig. 2. Scattering cross section (SCS) and multipole decomposition for a selection of incidence angles and polarizations: (a) for vertical incidence; (b)-(c) and (d)-(e) for incidence angles of 22.5° and 45°, respectively. The full numerical solution (dashed line, Full num.) is the SCS obtained from FDTD simulations.

Another approach is to solve the eigenvalue problem for Maxwell's source-free equations for the resonator material and geometry. As dielectric resonators have open boundaries, the Hamiltonian of the system is non-Hermitian and has complex eigenfrequencies. Such solutions are general for all open resonator systems, in nanophotonics they are commonly referred to as QNMs [7,24]. Given a set of eigenmodes within a spectral range, the scattering response is calculated through the excitation overlap with a source of choice. QNM gives the natural resonances within the scatterer and their corresponding near fields in a more intuitive representation [24]. Thus, the MPD and QNM techniques are complementary.

We begin by performing SCS simulations and calculating the MPD from the induced fields, illustrated in Fig. 2(a)-(e). We perform calculations for incidence angles of 6°, 22.5° and 45° and considered separately TE and TM polarized incident light, to match the experimental data (full SCS maps can be found in SI 2). The angular response of the SCS is similar to that of the specular reflectance in Fig. 1, even though the wavelength dip of the SCS is a bit shifted to 600 nm, which will be explained further on.

Optics EXPRESS

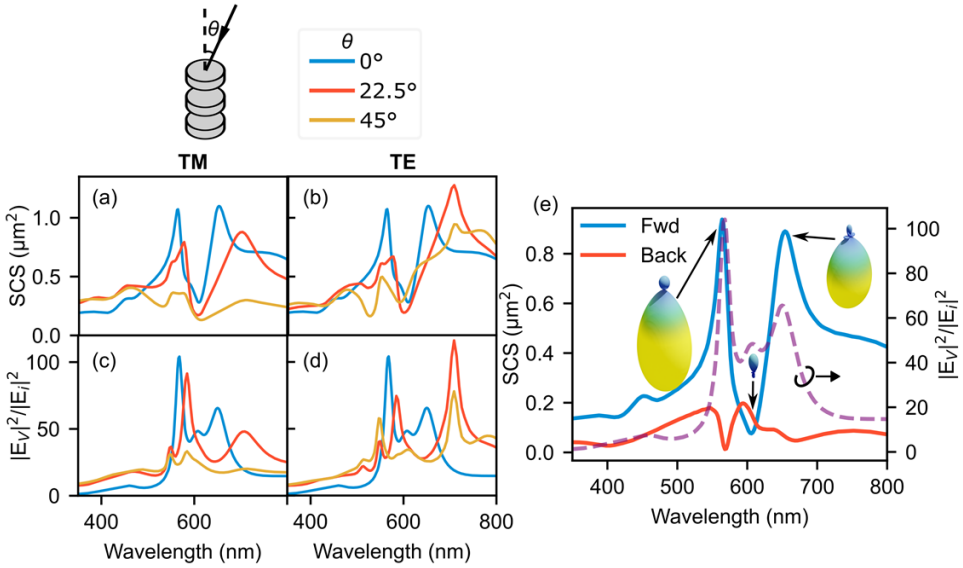

Fig. 3. Scattering cross section and enhancement of internal energy within the disks for select incidence angles (given in degrees) and polarization: (a) and (b), calculated SCS for TM and TE polarizations, respectively; (c) and (d), calculated internal energy for TM and TE polarizations, respectively; (e) SCS and internal energy for vertical incidence. In (e) the forward and backwards components of the SCS for normal incidence also includes insets of the far field radiation patterns at select wavelengths indicated by the arrows. The far field patterns are in scale with each other, size and brighter color indicates increased scattering.

The multipole decomposition here uses the spherical coordinate expansion with terms up to the electric and magnetic octupoles, which gives good agreement with the full numerical SCS. The MPD is calculated for the whole pillar as a single resonator. Thus, the resonator volume is relatively large and contains separate entities, which is why it can sustain higher order terms at these wavelengths. For spherical Mie particles one does not expect to see octupole contributions until larger diameters (~1.5 to 2 times the wavelength inside the material) [25]. Additionally, the individual disks in this structure are too small to sustain higher order resonances at the EDA wavelength, except for the magnetic MQ [18]. Thus, any higher order resonances for the three disk system stems from some combination of interacting EDA's or MQ's. As such the higher order resonances are longitudinal and less sensitive to polarization.

The MPD at normal incidence, Fig. 2(a), shows dips around a wavelength of 600 nm for all contributing terms, except for the magnetic octupole. In fact, the SCS show that the structure is close to the condition of a hybrid anapole (HA), where more than one of the terms and their toroidal counterparts cancel each other at the same wavelength [11]. As seen in the MPD for the higher angles, the spectral position of the individual dips can be tuned with the incidence angle, and at 22.5 ° most of the multipole dips overlap. Unfortunately, a magnetic octupole scattering contribution is present which prevents the total SCS from reaching even lower levels. To the best of our knowledge, an electric octupole anapole has not been reported in literature, although their existence is predicted.

A measure of the enhancement of the internal field is the volume averaged intensity. It is calculated by integrating the electric field intensity and normalized to the incoming field intensity and the resonator volume, $|\boldsymbol{E_v}|^2/|\boldsymbol{E_i}|^2 = \int_{\boldsymbol{V}} \epsilon_r |\boldsymbol{E}|^2 \boldsymbol{V} / \left(|\boldsymbol{E_i}|^2 \boldsymbol{V}\right)$. The result, seen in Fig. 3(a-d) together with the corresponding SCS in linear vertical scale, has three distinct peaks

Optics EXPRESS

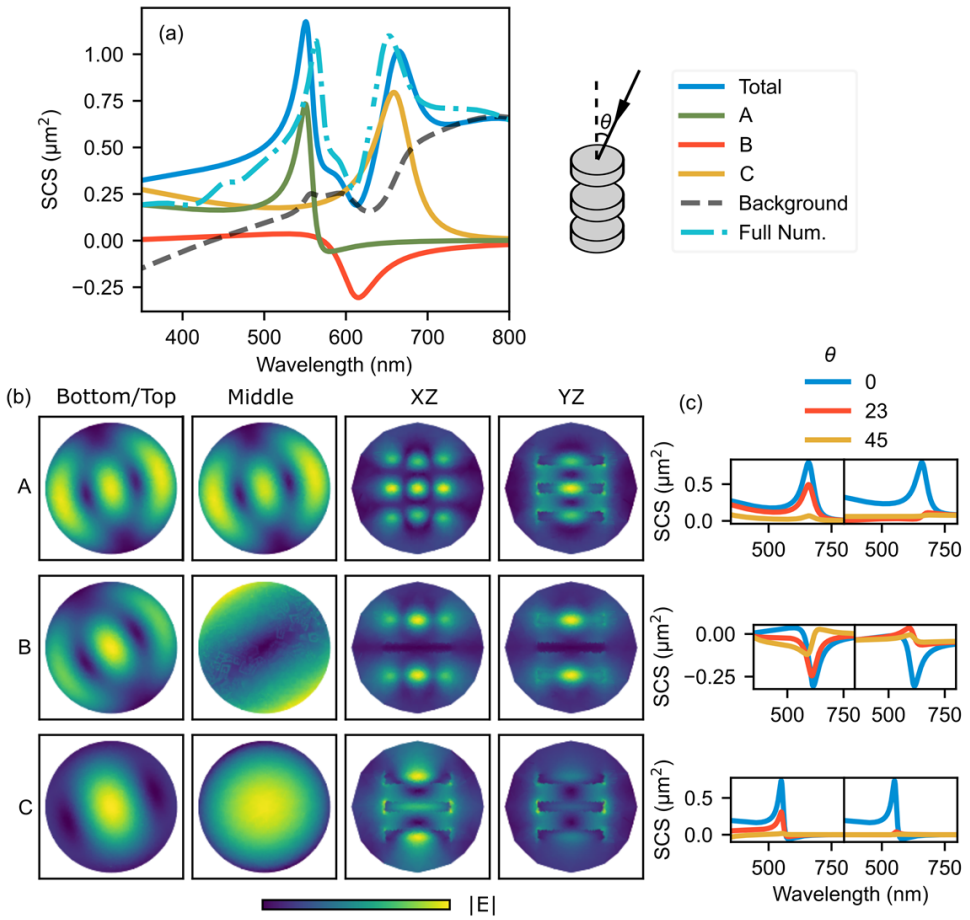

Fig. 4. SCS and Quasi-normal mode (QNM) breakdown for the three-disk system. The three most significant eigenmodes of the system are labelled A,B and C, for convenience. (a) Calculated SCS for vertical incidence. (b) Field plots for the modes in the respective disks in the stack. The field plots are normalized to the respective highest value in each mode for clarity. The Bottom/Top column of field plots are representative of both disks since the system is symmetric around the middle disk. (c) The evolution of the contribution to the total SCS of the individual modes (A, B and C) for three selected incidence angles (in degrees).

for normal incidence. The three peaks each coincide with either a peak or a dip in the SCS. As the incidence angle increases the peaks split further apart in wavelength, especially for the TE polarized incidence (Fig. 3(b,d)), consistent with the additional peaks seen in the experimental data (Fig. 1(c)). Further, we show that the peaks in the total SCS are associated with forward scattering. Notably the initial peak at 580 nm is forward scattered with the backscattering reaching zero. The dip in backscattering coincides with the dip observed in the experimental data in Fig. 1 and the dip in electric octupole contribution in Fig. 2(a). Thus, the dip associated with anapole excitation in experiment is due to hybridized anapoles forming an electric octupole anapole which forward scatters into the substrate. In theory, an anapole excitation should be non-radiating and not scatter, i.e. the SCS should be zero at that point. However, the hybridized anapoles creates additional radiation channels that enable the forward scattering. Yet, the energy confinement is highest at the strong forward scattering peak.

Optics EXPRESS

To further investigate the response of the pillars we employ QNM analysis, presented in Fig. 4. The QNM solutions are generated with COMSOL and a modified version of the software package MAN [21]. There are an infinite amount of solutions to the eigenvalue problem, however only a few will have significant contributions in the wavelength region of interest. In this case we have calculated 200 solutions closest to wavelength 600 nm, where the three with highest contribution are plotted separately, and the rest treated as background. We use a constant refractive index of 3.4 for the disks, which corresponds to $Al_{0.7}$ $Ga_{0.3}As$ at a wavelength of 600 nm. At normal incidence (Fig. 4(a)), the response can be attributed to three eigenmodes of the system, here labelled A,B and C. A contributes to the peak in the SCS before the dip, however the fields associated with this mode is that of an anapole in all three disks (Fig. 4(b)). It can also be seen that this mode is the one corresponding to the first and highest peak in the internal energy enhancement of Fig. 3(c,d) and the forward scattering in Fig. 3(e), and thus the electric octupole dip in Fig. 2(a), i.e. three stacked EDAs form an electric octupole anapole. Mode B contributes to the dip; however it is only the top and bottom disk that displays anapole patterns, the middle disk is nearly void of internal electric field (Fig. 4(b)). In fact mode A and B are hybridized modes of the single disk anapole. Mode C is longitudinal (Fig. 4(b)) and contributes to the scattering at wavelengths beyond the dip position. The three mode contributions to the total SCS decreases with incidence angle and at 45° they are flat (Fig. 4(c)). For higher incidence angles other modes dominate the response.

4. Conclusions

We have shown how a system of stacked III-V disks supporting hybridized anapoles evolves with incidence angle and polarization using two separate but complementary analysis techniques. We find that the stacked geometry shows hybridized anapole excitation for a broad span of incidence angles, with tunability of the individual multipolar response up to octupoles, including an electric octupole anapole, and we show how the average confined energy varies under angled excitation. The study shows that focusing optics can excite the high energy resonances with a large portion of its power, increasing the in-coupling term for non-linear applications.

Funding. Vetenskapsrådet (2019-05321).

Acknowledgments. The authors thank Prof. Lars Österlund, Uppsala University, for access to the spectrophotometer.

Disclosures. The authors declare no conflicts of interest.

Data availability. Data underlying the results in this paper are available upon request.

Supplemental document. See Supplement 1 for supporting content.

References

1. S. Liu, M. B. Sinclair, S. Saravi, *et al.*, "Resonantly Enhanced Second-Harmonic Generation Using III-V Semiconductor All-Dielectric Metasurfaces," Nano Lett. **16**(9), 5426–5432 (2016).
2. S. Jahani and Z. Jacob, "All-dielectric metamaterials," Nat. Nanotechnol. **11**(1), 23–36 (2016).
3. K. Koshelev, S. Kruk, E. Melik-Gaykazyan, *et al.*, "Subwavelength dielectric resonators for nonlinear nanophotonics," Science **367**(6475), 288–292 (2020).
4. A. Lochbaum, Y. Fedoryshyn, A. Dorodnyy, *et al.*, "On-Chip Narrowband Thermal Emitter for Mid-IR Optical Gas Sensing," ACS Photonics **4**(6), 1371–1380 (2017).
5. J. Tian, Q. Li, P. A. Belov, *et al.*, "High- Q All-Dielectric Metasurface: Super and Suppressed Optical Absorption," ACS Photonics **7**(6), 1436–1443 (2020).
6. Z. Wang, G. Hu, X. Wang, *et al.*, "Single-layer spatial analog meta-processor for imaging processing," Nat. Commun. **13**(1), 2188 (2022).
7. L. Huang, L. Xu, D. A. Powell, *et al.*, "Resonant leaky modes in all-dielectric metasystems: Fundamentals and applications," Phys. Rep. **1008**, 1–66 (2023).
8. Y. Kivshar, "The Rise of Mie-tronics," Nano Lett. **22**(9), 3513–3515 (2022).
9. Y. Yang and S. I. Bozhevolnyi, "Nonradiating anapole states in nanophotonics: From fundamentals to applications," Nanotechnology **30**(20), 204001 (2019).
10. K. J. Vahala, "Optical microcavities," Nature **424**(6950), 839–846 (2003).

Optics EXPRESS

11. A. Canós Valero, E. A. Gurvitz, F. A. Benimetskiy, *et al.*, "Theory, Observation, and Ultrafast Response of the Hybrid Anapole Regime in Light Scattering," Laser Photonics Rev. **15**(10), 1–14 (2021).
12. A. E. Miroshnichenko, A. B. Evlyukhin, Y. F. Yu, *et al.*, "Nonradiating anapole modes in dielectric nanoparticles," Nat. Commun. **6**(1), 8069 (2015).
13. L. Huang, L. Xu, M. Rahmani, *et al.*, "Pushing the limit of high-Q mode of a single dielectric nanocavity," Adv. Photonics **3**(01), 016004 (2021).
14. M. V. Rybin, K. L. Koshelev, Z. F. Sadrieva, *et al.*, "High- Q Supercavity Modes in Subwavelength Dielectric Resonators," Phys. Rev. Lett. **119**(24), 243901 (2017).
15. A. A. Basharin, E. Zanganeh, A. K. Ospanova, *et al.*, "Selective superinvisibility effect via compound anapole," Phys. Rev. B **107**(15), 155104 (2023).
16. E. Bulgakov, K. Pichugin, and A. Sadreev, "Mie resonance engineering in two disks," Photonics **8**(2), 49 (2021).
17. K. Pichugin, A. Sadreev, and E. Bulgakov, "Ultrahigh-Q system of a few coaxial disks," Nanophotonics **10**(17), 4341–4346 (2021).
18. F. Vennberg, A. P. Ravishankar, and S. Anand, "Manipulating light scattering and optical confinement in vertically stacked Mie resonators," Nanophotonics **11**(21), 9492 (2022).
19. S. Tian, J. Wang, S. Sun, *et al.*, "The anapole state excited by an oblique incidence," Phys. Scr. **98**(8), 085515 (2023).
20. L. Fornasari, M. Passoni, F. Marabelli, *et al.*, "Angular dependence and absorption properties of the anapole mode of Si nano-disks," J. Appl. Phys. **129**(2), 023102 (2021).
21. W. Yan, R. Faggiani, and P. Lalanne, "Rigorous modal analysis of plasmonic nanoresonators," Phys. Rev. B **97**(20), 205422 (2018).
22. R. Alaee and C. Rockstuhl, "An electromagnetic multipole expansion beyond the long-wavelength approximation," 1–21 (n.d.).
23. R. Alaee, C. Rockstuhl, and I. Fernandez-Corbaton, "Exact Multipolar Decompositions with Applications in Nanophotonics," Adv. Opt. Mater. **7**(1), 1–14 (2019).
24. P. Lalanne, W. Yan, K. Vynck, *et al.*, "Light Interaction with Photonic and Plasmonic Resonances," Laser Photonics Rev. **12**(5), 1–38 (2018).
25. E. A. Gurvitz, K. S. Ladutenko, P. A. Dergachev, *et al.*, "The High-Order Toroidal Moments and Anapole States in All-Dielectric Photonics," Laser Photonics Rev. **13**(5), 1–13 (2019).